

# Graphitization behavior of polymer in the gelcasted alumina by sintering

Tomoaki KATO, Takashi SHIRAI, Masayoshi FUJI<sup>†</sup> and Minoru TAKAHASHI

Ceramics Research Laboratory, Nagoya Institute of Technology, 3-101-1, Honmachi, Tajimi, Gifu 507-0033

**A new fabrication method of electrical conductive alumina/carbon composite ceramics has been investigated. An advantage of this material is good electrical conductivity based on the uniformity of carbon network generated from polymer in the gelcasted green body. In this study, we discussed the graphitization behavior of the polymer into a gelcasted alumina. As a result of the graphitization, the density, electrical conductivity and degree of graphitization were increasing at a higher temperature. Especially, those values were remarkably increased from 1500°C. The sample sintered at 1700°C, it has an electrical conductivity of 4.11 S/cm and high graphitization similar to pyrolytic graphite. It is thought that the presence and sintering of alumina particle has an important factor in this behavior.**

©2009 The Ceramic Society of Japan. All rights reserved.

Key-words : Electrical conductivity, Gelcasting, Carbon, Graphitization

[Received May 12, 2009; Accepted August 20, 2009]

## 1. Introduction

Recently, there had been various proposed methods in fabricating an electrical conductive ceramics. Some of this common method in improving the electrical properties for an insulating ceramics is incorporating electrically conductive fillers such as metals,<sup>1)</sup> metallic oxides<sup>2)</sup> or carbon. However, in order to achieve the desired level of electrical properties, usually high percentage of fillers was added to the composite material but in this case loading or the mechanical properties might deplete or cause great effect on the physico chemical properties of the ceramic/composite materials such as the refractoriness, hardness and stiffness. Hence, the reduction or small amount of additive/filler is desired. To lessen these problems, a nano-carbon fiber was introduced as fillers in the composite system.<sup>3)-7)</sup> Carbon-nanotubes (CNTs) have an advantage as conductive filler, which includes high tensile strength, electrical conductivity, low density and large surface area. However, CNTs have strong coagulation properties due to the strong attractive force of the van der Waals in each CNTs particles.<sup>7)</sup> Coagulated fillers can cause defects of ceramics matrix that could eventually decrease in the mechanical property of the composite material. To reduce this occurrence, various studies have been developed in preventing coagulation of CNTs particles.<sup>3),8)</sup>

A new approached of fabricating alumina/carbon network composite material by combination of gel-casting method<sup>9)</sup> and sintering under inert atmosphere<sup>10),11)</sup> had been developed in our group. In this method, the uniform polymer network is generated from the monomer dissolved into the slurry during gelcasting process, inducing a precursor of carbon. Then, the resultant carbon exists homogeneously around each alumina particles. Therefore, the homogeneous carbon that is less than 1 wt% in the ceramics matrix can induce a high and homogeneous electrical conductivity to the composite material.

Generally, induced electrical property of composite material fabricated by mixing with conductive filler is greatly affected by

the property of fillers, hence, an investigation between them should be studied.

In previous works,<sup>11)</sup> it is confirmed by electron diffraction that the carbon in the alumina matrix sintered at 1700°C has a graphite structure. However, the graphitization process is not yet investigated. The degree of graphitization is an important factor for the electrical property of graphite carbon materials. In this study, it aims to clarify the graphitization behavior of polymer in the alumina matrix under sintering process, and the effect of the degree of graphitization on electrical conductivity is investigated.

## 2. Experimental

### 2.1 Sample preparation

The materials used in this study were shown in **Table 1**. An alumina powder of mean particle diameter 0.5  $\mu\text{m}$  (AL160-SG4, Showa Denko Co., Yokohama, Japan) was used as a resource of the ceramics matrix. Methacryamide and N,N'-Methylene-bis-acrylamide were dissolved in a distilled water as gellants. The alumina powder was dispersed to the solvent with a dispersant (Seruna D-305, an ammonium salt of polycarboxylate solution, Chukyo Yushi, Japan) by ball milling for 24 h. The well dispersed slurry was agitated under a vacuum condition for 15 min to degas. Then, ammonium persulfate solution of 10 mass% and N,N,N',N'-Tetramethylethylenediamine were added to the slurry in order to have a polymerization reaction. The initiated slurry was poured into the mold until solidifies for 12 h. The solidified

Table 1. Composition of Alumina Slurry Obtained by Gelcasting

Kinds of starting materials	Composition (mass%)
alumina	80.0
distilled water	15.1
dispersant	0.720
methacrylamide	3.15
N,N'-methylenebis- acrylamide	1.05

<sup>†</sup> Corresponding author: M. Fuji; E-mail: fuji@nitech.ac.jp

wet green bodies were demolded and dried at 25°C for 5 d under controlled humidity from 90% to 60%. The dried green-body was sintered at 900, 1100, 1200, 1300, 1400, 1500 and 1700°C for 2 h under argon atmosphere at 150 kPa.

## 2.2 Characterization

The apparent density of sintered bodies was measured by Archimedes method.

The cutting surface of sintered bodies was observed by scanning electron microscopy (SEM) (JSM-7000F, JEOL Ltd.). These samples were observed without conductive coating.

Electrical conductivity was measured by 4-probe method by using DC voltage current source/monitor (R6243, Advantest, Japan). In this measurement, the probe current was fixed to 0.1 mA.

The carbon content in green body and sintered body was measured by Carbon Combustion Analyzer (EMIA-110, Horiba, Ltd.).

Raman spectroscopy for analysis of the carbon in the sintered body was recorded over the frequency ranging from 1000 to 2000  $\text{cm}^{-1}$  at an interval of 1.86  $\text{cm}^{-1}$  with collection time of 10 s (Laser Raman Spectrometer NRS-3100, JASCO Co.). A 532 nm laser beam of 11 mW was used as excitation source.

## 3. Results and discussion

**Figure 1** shows the apparent density of the alumina carbon composite material at each sintering temperature. It was clearly shown that the density was constant around 2.20  $\text{g}/\text{cm}^3$  up to 1300°C but dramatically increased when the sintering temperature reached from 1500 to 1700°C. This resulted to 2.85  $\text{g}/\text{cm}^3$  as the highest density at 1700°C.

While in **Fig. 2**, the SEM images of sintered samples at each sintering temperature was shown. The image of sintered sample at 900°C was not able to be taken because the low electrical conductivity as described later. The change in the grain size was not seen in (a) and (b) that was sintered below 1300°C. The grain growth was confirmed at 1500°C, which becomes clearer at 1700°C. This tendency of grain growth is similar as the increasing of apparent density shown in Fig. 1.

The electrical conductivity of sintered sample was shown in **Fig. 3**. The sintered sample at 900°C has a very low quality of electrical conduction so it was not shown in this study. But the sintered samples at more than 900°C were shown in Fig. 3. Based on the graph alone, one can observed that the electrical

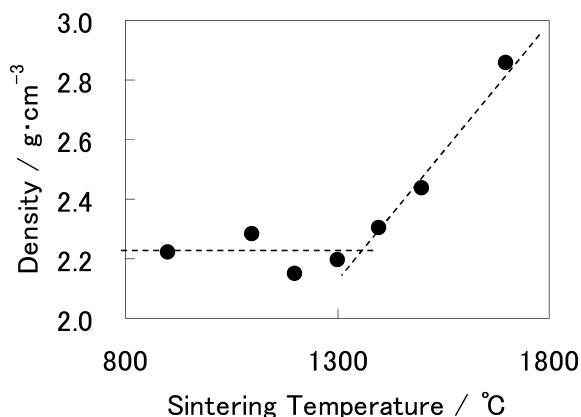


Fig. 1. Density of alumina/carbon composite ceramics as a function of sintering temperature.

conductivity linearly increased at elevated sintering temperature especially above 1500°C.

From the results of the carbon content measurement as shown in **Table 2**, the carbon content in the sintered body was almost same regardless of the sintering temperature, and the carbon residue rate was about 25%. The elimination and the carbonization of the polymer in green body were completed at less than 900°C. The carbon residue ratio was calculated as a ratio of the carbon content in the green body and that in the sintered body. The calculated value based on the slurry component is 2.95 mass% similar to the measured value. These results indicate that the occurrence of electrical conductivity at 1100°C and the conductivity change of increasing rate at 1500°C are not given by the

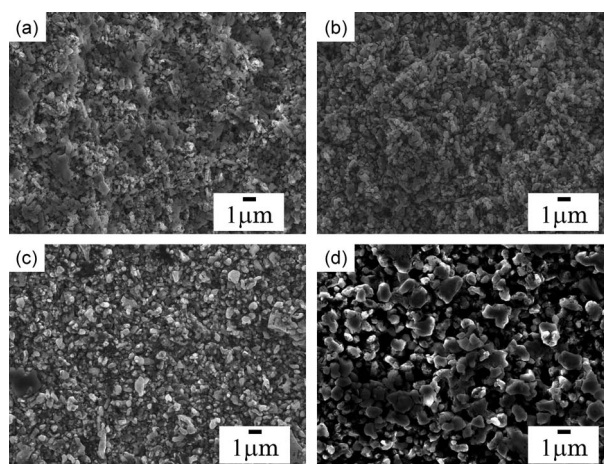


Fig. 2. SEM images of the cutting surface of sintered sample at each sintering temperature; a) 1100°C, b) 1300°C, c) 1500°C, d) 1700°C.

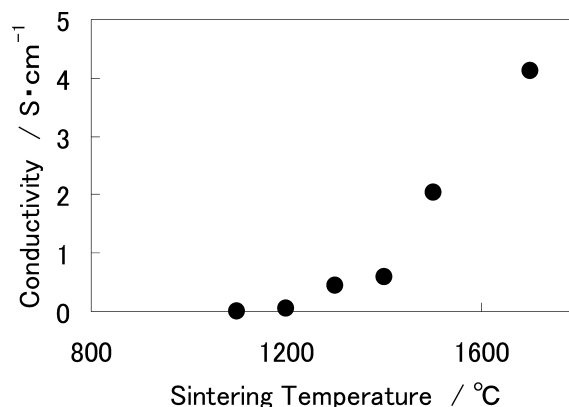


Fig. 3. Electrical conductivity of alumina/carbon composite ceramics as a function of sintering temperature.

Table 2. Carbon Content in Sintered Samples

Sintering temp.	Carbon content (mass%)
900°C	0.78
1100°C	0.70
1300°C	0.77
1500°C	0.78
(green body)	3.1

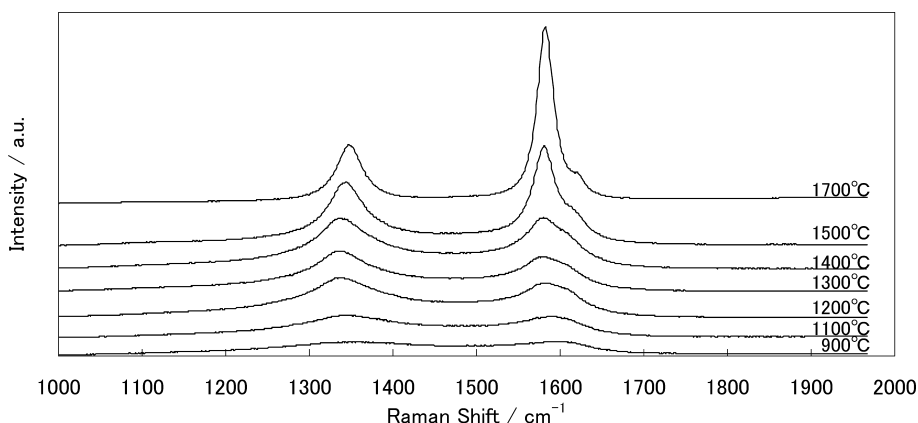


Fig. 4. Raman spectrum of sintered sample at each sintering temperature.

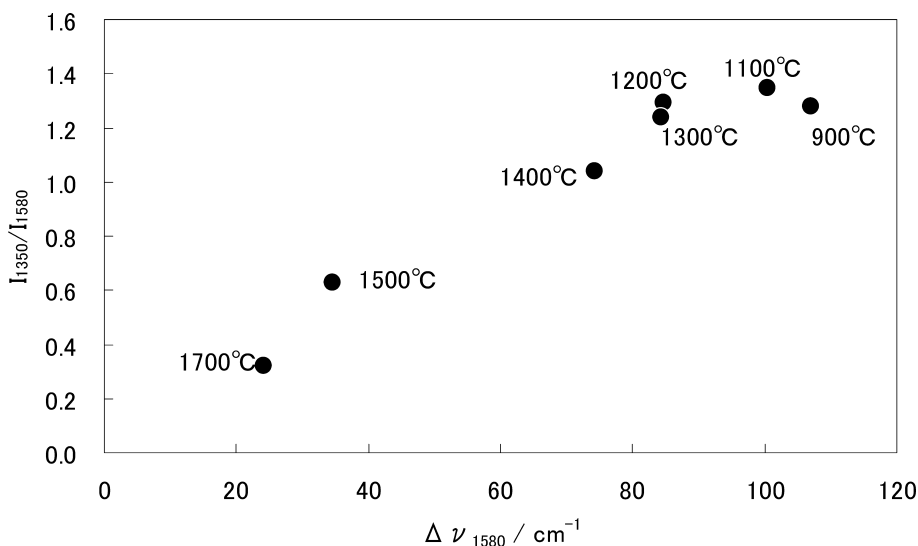


Fig. 5. Correlation plot between the  $\Delta\nu_{1580}$  and  $I_{1360}/I_{1580}$ .

change of the carbon content. These can be further explaining using the Raman spectroscopy measurement.

The result of a measurement by Raman spectroscopy was shown in Fig. 4. Two characteristic peaks of the graphite structure appeared according to increasing of sintering temperature. One of the peaks around  $1360\text{ cm}^{-1}$  was called D-band while the other was called G-band at  $1580\text{ cm}^{-1}$ .<sup>12,13)</sup> The increasing and the sharpening of G-band above  $1500^\circ\text{C}$  were remarkable. The D-band was known as the disorder-induced Raman peak. This peak indicates the existence of defect or edge plane on graphite structure. The G-band is induced by basal plane of graphite structure. These two peaks were usually used for estimation of graphite structure. An intensity ratio of D-band and G-band ( $I_{1360}/I_{1580}$ ) indicates the degree of graphitization. The half band width of G-band ( $\Delta\nu_{1580}$ ) showed the crystallinity and turbostraticity of graphite planes. These values decrease with the progress of graphitization. A correlation plot between the  $\Delta\nu_{1580}$  and  $I_{1360}/I_{1580}$  was shown in Fig. 5. The graphite structure of the carbon content was guessed from a relative position in this plot. It was thought that the structure of the graphite has changed from amorphous into the turbostratic structure with small graphite plane between  $900^\circ\text{C}$  and  $1300^\circ\text{C}$  because almost  $I_{1360}/I_{1580}$  constant and  $\Delta\nu_{1580}$  decrease. At  $1400^\circ\text{C}$ , the progress of graphitiza-

tion can be confirmed, because the value of  $I_{1360}/I_{1580}$  starts decreasing. The progress of graphitization becomes more remarkable at  $1500^\circ\text{C}$ , and the growth of the graphite plane and the improvement of the orientation were seen in the graph. At  $1700^\circ\text{C}$ ,  $I_{1360}/I_{1580}$  and  $\Delta\nu_{1580}$  indicates 0.32 and 24.1, and it was similar to the edge side of the pyrolytic graphite.<sup>14)</sup>

The increasing of electrical conductivity by the improvement of the degree of graphitization was well known. It is confirmed that the increase in the degree of graphitization was shown in the Raman analysis and that the electrical conductivity can be improved greatly at  $1500^\circ\text{C}$ .

In general graphitization from polymers, high temperature about  $3000^\circ\text{C}$  is needed to improve the graphitization.<sup>15)</sup> However, the progress of graphitization in this study was given at lower temperature. Otani et al. have reported about catalytic graphitization of carbon by various metals.<sup>16,17)</sup> They reported about catalytic effects such as carbide formation-decomposition, dissolution of carbon to the metals, removal of strain by oxidation reaction and other effects. In previous study, the existence of the aluminum carbide in the sintered body was confirmed by the XPS measurement, and there is a possibility of the catalytic carbonization effect by this carbide. However, the catalytic graphitization in Otani's study was reported on more high tem-

perature above 2000°C. The sintering temperature of 1700°C of the sample is too low for inducing graphitization. The accelerating effect of pressure in the graphitization reported by Inagaki et al.<sup>18)</sup> is thought as another reason for high degree of graphitization on the sintered body. Because the progress of the sintering shown in an increase of the density and the increase of the degree of graphitization were synchronal at more than 1500°C, the reorientation of graphite plane on the alumina grain boundary might have been promoted by the local pressure of alumina sintering.

#### 4. Conclusion

The graphitization behavior of polymer in the gelcasted green body under sintering process was discussed. The progress of graphitization was given at lower temperature than the temperature for graphitization of the common carbon materials that led to the increase of electrical conductivity. The resultant graphite at 1700°C has a similar structure of the edge surface of pyrolytic graphite. It is considered that the high degree of graphitization is given by the catalytic graphitization of alumina particle and pressure graphitization by sintering.

**Acknowledgement** This research was carried out by the Ministry of Education, Culture, Sports, Science, and Technology (MEXT) financed project “Cooperation for Innovation Technology and Advanced Research in Evolution Area”.

#### References

- 1) S. Hussain I. Barbariol, S. Roitti and O. Sbaizero, *J. Eur. Ceram. Soc.*, **23**, 315–321 (2002).
- 2) C. Laurent, A. Peigney, O. Dumortier and A. Rousset, *J. Eur. Ceram. Soc.*, **18**, 2005–2013 (1998).
- 3) J. Fan, D. Zhao, M. Wu, Z. Xu and J. Song, *J. Am. Ceram. Soc.*, **89**, 750–753 (2006).
- 4) K. Ahmad, W. Pan and S. Shi, *Appl. Phys. Lett.*, **89**, 133122 (2006).
- 5) K. Hirota, Y. Takaura, M. Kato and Y. Miyamoto, *J. Mater. Sci.*, **42**, 4792–4800 (2007).
- 6) G. Yamamoto, M. Omori, T. Hashida and H. Kimura, *Nanotechnology*, **19**, 315708 (2008).
- 7) J. Chen, M. A. Hamon, H. Hu, Y. Chen, A. M. Rao, P. C. Eklund and R. C. Haddon, *Science*, **282**, 95–98 (1998).
- 8) K. Hernadi, E. Couteau, J. W. Seo and L. Forro, *Langmuir*, **19**, 7026–7029 (2003).
- 9) O. O. Omatete, M. A. Janney and R. A. Strehlow, *Am. Ceram. Soc. Bull.*, **70**, 1641–1649 (1991).
- 10) R. L. Menchavez, M. Fuji, T. Yamakawa, T. Endo and M. Takahashi, *Mater. Sci. Forum*, **561–565**, 2123–2126 (2007).
- 11) R. L. Menchavez, M. Fuji and M. Takahashi, *Adv. Mater.*, **20**, 2345–2351 (2008).
- 12) F. Tuinstra and J. L. Koenig, *J. Chem. Phys.*, **53**, 1126–1130 (1969).
- 13) P. Lespade, R. Al-Jishi and M. S. Dresselhaus, *Carbon*, **20**, 427–431 (1982).
- 14) Y. Wang, D. C. Alsmeyer and R. C. McCreery, *Chem. Mater.*, **2**, 557–563 (1990).
- 15) M. Minus and S. Kumar, *JOM*, **57**, 52–58 (2005).
- 16) A. Oya, M. Mochizuki and S. Otani, *Carbon*, **17**, 71–76 (1978).
- 17) A. Oya and S. Otani, *Carbon*, **17**, 131–137 (1978).
- 18) T. Noda, K. Kamiya and M. Inagaki, *Bull. Chem. Soc. Japan*, **41**, 485–492 (1968).